ISSN 1070-3284, Russian Journal of Coordination Chemistry, 2019, Vol. 45, No. 3, pp. 188–199. © Pleiades Publishing, Ltd., 2019.
Russian Text © A.V. Piskunov, O.Yu. Trofimova, A.V. Maleeva, A.V. Cherkasov, 2019, published in Koordinatsionnaya Khimiya, 2019, Vol. 45, No. 3, pp. 158–169.

Template Synthesis of Tin(IV) Complexes with Tridentate Iminopyridine Ligands

A. V. Piskunov[a], *, O. Yu. Trofimova[a], A. V. Maleeva[a], and A. V. Cherkasov[a]

[a] *Razuvaev Institute of Organometallic Chemistry, Russian Academy of Sciences, Nizhny Novgorod, 603950 Russia*

**e-mail: pial@iomc.ras.ru*

Received June 20, 2018; revised August 24, 2018; accepted September 5, 2018

Abstract—Six-coordinate metal complexes containing tridentate Schiff bases with an ONN-chelating moiety were prepared by template synthesis on tin tetrachloride using various aminophenols and α-carbonyl-substituted pyridines. The structures of five compounds were studied by X-ray diffraction (CIF files CCDC nos. 849152–1849156). The UV/Vis spectra of the obtained series of compounds were found to be highly sensitive to the nature of substituents in the moieties of organic ligand.

Keywords: tin(IV) complexes, substituted aminophenols, Schiff bases, redox active iminopyridine ligands template synthesis

DOI: 10.1134/S1070328419020040

INTRODUCTION

Schiff bases are highly popular ligand systems widely used in the design of coordination compounds [1]. Most often, they are used to construct transition metal complexes [2]. However, in recent years, this type of organic ligands have been often used in the chemistry of main group elements [3]. In particular, the coordination chemistry of tin(IV) is vigorously developing. Analysis of the recent literature shows a surge of research in this area. Apart from high diversity of structural types of tin(IV) coordination compounds that are based on Schiff bases [4, 5], the number of applied problems that can be solved using complexes of this type is permanently increasing. They include a broad range of biologically active agents possessing antimicrobial [6], cytotoxic [7–9], bactericidal [10], antifungal [11], DNA-directed chemotherapeutic [12, 13], anti-inflammatory [14], and antituberculosis [15] types of action. New fluorescent biomarkers [7], luminescent materials [16, 17], fine organic synthesis catalysts [18, 19], and components for nonlinear optics materials [20] have been obtained.

Tridentate Schiff bases containing an iminopyridine moiety and a phenol group capable of covalent binding to a metal are promising ligands combining the polydentate function and potentially biologically active groups. Complexes of both transition (Ni [21], Cu [22–25], Mn [26, 27], Co [22], Fe [28–30], Zn [21, 22, 31], Cd [21, 31]) and main group (Pb [32]) elements have been prepared with ligands of this type. Tin compounds with these ligands are at the center of attention of many researchers due to their structural diversity and potential applications [33–35]. It was shown [36] that pentadentate ligands containing an iminopyridine moiety are successfully assembled in the tin coordination sphere. This communication describes the template synthesis of a series of tin(IV) complexes (**I**–**XIX**) containing various tridentate Schiff bases from substituted *o*-aminophenols and α-carbonyl-substituted pyridines with participation of tin tetrachloride.

EXPERIMENTAL

The following commercial chemicals were used: 2-pyridinecarboxaldehyde (Aldrich), 2-benzoylpyridine (Aldrich), 2-acetylpyridine (Aldrich), $SnCl_4$ (Aldrich), 4,6-di-*tert*-butyl-*o*-aminophenol (Aldrich), 4-methyl-*o*-aminophenol (Aldrich), 5-methyl-*o*-aminophenol (Aldrich), 4-*tert*-butyl-*o*-aminophenol (Aldrich), 4-chloro-*o*-aminophenol (Aldrich), 4-nitro-*o*-aminophenol (Aldrich), and 6-chloro-4-nitro-*o*-aminophenol (Aldrich). The reagent grade and analytical grade solvents were dried by standard procedures [37].

IR spectra were measured on an FSM-1201 FT IR spectrometer (mineral oil mulls; KBr cells). NMR spectra were recorded in $CDCl_3$ (**I**, **VIII**, **X**, **XI**, **XII**, and **XV**) and $(CD_3)_2CO$ (**II**, **III**, **IV**, **V**, **VI**, **IX**, **XIII**, **XIV**, **XVI**, **XVII**, **XVIII**, **XIX**) on a Bruker Avance III NMR spectrometer (400 MHz) with Me_4Si as the internal standard. UV/Vis spectra were measured on Perkin-Elmer Lambda 25 and SHIMADZU UV-3600 spectrometers.

Synthesis of complexes I–XIX. All operations on the synthesis and investigation of tin complexes with

tridentate ONN-ligands were carried out under aerobic conditions. A solution of 2-pyridinecarboxaldehyde (**I**–**VII**) (or 2-benzoylpyridine (**VIII**–**XIV**), 2-acetylpyridine (**XV**–**XIX**)) (1 mmol) and 4,6-di-*tert*-butyl-*o*-aminophenol (**I**, **VIII**, **XV**) (or any of 4-methyl-*o*-aminophenol (**II**, **IX**, **XVI**), 5-methyl-*o*-aminophenol (**III**, **X**, **XVII**), 4-*tert*-butyl-*o*-aminophenol (**IV**, **XI**, **XVIII**), 4-chloro-*o*-aminophenol (**V**, **XII**, **XIX**), 4-nitro-*o*-aminophenol (**VI**, **XIII**), and 6-chloro-4-nitro-*o*-aminophenol (**VII**, **XIV**)) (1 mmol) in methanol (15 mL) were added with stirring at 50°C to a solution of tin tetrachloride (1 mmol) in methanol (30 mL). The color of the reaction mixture gradually changed during 15 min. The stirring was continued for 6 h, which resulted in quantitative precipitation of the target complex as a finely crystalline solid. The crystals of complexes **I**, **VIII**, **IX**, **X**, and **XII** suitable for X-ray diffraction were obtained by slow evaporation of methanol solutions of the compounds.

2,4-Di-*tert*-butyl-6-((pyridin-2-ylmethylene)amino)phenolatotrichlorotin(IV) (**I**): violet crystals, 70% yield.

For $C_{20}H_{25}N_2OCl_3Sn$

Anal. calcd., %	C, 44.88	H, 4.86	Cl, 19.93
Found, %	C, 45.01	H, 4.99	Cl, 19.72

IR (ν, cm^{-1}): 1608 s, 1598 s, 1530 s, 1478 s, 1445 s, 1363 s, 1297 s, 1275 s, 1243 s, 1197 s, 1161 s, 920 s, 862 s, 827 s, 765 s.

^1H NMR ($CDCl_3$; 293 K; δ, ppm): 1.32 (s, 9H, *t*-Bu), 1.48 (s, 9H, *t*-Bu), 7.33 (d, J = 2.1 Hz, $1H_{ar}$), 7.54 (d, J = 2.1 Hz, $1H_{ar}$), 7.84 (m, $1H_{Py}$), 8.02 (d, J = 7.8 Hz, $1H_{Py}$), 8.29 (td, J = 7.8 Hz, J = 1.3 Hz, $1H_{Py}$), 8.64 (s, J ($^{119}Sn-^1H$) = 98.3 Hz, C–H), 9.12 (d, J = 5.1 Hz, J ($^{119}Sn-^1H$) = 25.4 Hz, $1H_{Py}$); ^{13}C NMR ($CDCl_3$; 293 K; δ, ppm): 29.2 (CH_3(*t*-Bu)), 30.1 (CH_3(*t*-Bu)), 35.1 (C(*t*-Bu)), 35.6 (C(*t*-Bu)), 110.6, 123.2, 128.0, 128.2, 131.8, 133.0, 141.5, 141.7, 142.8, 142.9, 145.9 (C_{arl}), 157.3 (C=N); ^{119}Sn NMR ($CDCl_3$; 293 K; δ, ppm): –514.

UV (λ, nm (ε, L cm^{-1} mol^{-1})), acetonitrile: 367 (10979), 494 (7456); toluene: 378 (13370), 522 (10750); methanol: 369 (10690), 497 (7650); diethyl ether: 373 (13970), 515 (10550); dichloromethane: 381 (10440), 521 (10440).

4-Methyl-2-((pyridin-2-ylmethylene)amino)phenolatotrichlorotin(IV) (**II**): red-violet finely crystalline powder, 72% yield.

For $C_{13}H_{11}N_2OCl_3Sn$

Anal. calcd., %	C, 35.79	H, 2.54	Cl, 24.38
Found, %	C, 35.81	H, 2.45	Cl, 24.32

IR (ν, cm^{-1}): 1606 s, 1540 s, 1489 s, 1290 s, 1276 s, 1242 s, 1211 s, 1149 s, 881 s, 819 s, 812 s, 778 s.

^1H NMR ($(CD_3)_2CO$); 293 K; δ, ppm): 2.32 (s, 3H, CH_3), 6.94 (d, J = 8.5 Hz, $1H_{ar}$), 7.34 (dd, J = 2.4 Hz, J = 8.5 Hz, $1H_{ar}$), 7.73 (s, $1H_{ar}$), 8.27 (m, $1H_{Py}$), 8.53 (m, $1H_{Py}$), 8.70 (td, J = 7.8 Hz, J = 1.3 Hz, $1H_{Py}$), 9.18 (d, J = 5.3 Hz, $1H_{Py}$), 9.52 (s, 1H, C–H); ^{119}Sn NMR ($(CD_3)_2CO$); 293 K; δ, ppm): –513.

UV (λ, nm (ε, L cm^{-1} mol^{-1})): acetonitrile: 350 (10729), 480 (7518).

5-Methyl-2-((pyridin-2-ylmethylene)amino)phenolatotrichlorotin(IV) (**III**): red finely crystalline powder, 69% yield.

For $C_{13}H_{11}N_2OCl_3Sn$

Anal. calcd., %	C, 35.79	H, 2.54	Cl, 24.38
Found, %	C, 35.92	H, 2.75	Cl, 24.12

IR (ν, cm^{-1}): 1602 s, 1588 s, 1537 s, 1485 s, 1298 s, 1285 s, 1244 s, 1157 s, 1125 s, 925 s, 902 s, 806 s, 806 s, 799 s, 773 s, 730 s.

^1H NMR ($(CD_3)_2CO$); 293 K; δ, ppm): 2.36 (s, 3H, CH_3), 6.77 (d, J = 8.4 Hz, $1H_{ar}$), 6.87 (s, $1H_{ar}$), 7.87 (d, J = 8.4 Hz, $1H_{ar}$), 8.25 (m, $1H_{Py}$), 8.50 (m, $1H_{Py}$), 8.69 (m, $1H_{Py}$), 9.16 (d, J = 5.1 Hz, $1H_{Py}$), 9.47 (s, J ($^{119}Sn-^1H$) = 108.6 Hz, C–H); ^{13}C NMR ($(CD_3)_2CO$); 293 K; δ, ppm): 21.2 (CH_3); 118.4, 119.8, 120.3, 129.7, 130.2, 136.3, 138.3, 144.5, 145.6, 147.1, 147.4 (C_{ar}); 157.1 (C=N); ^{119}Sn NMR ($(CD_3)_2CO$); 293 K; δ, ppm): –513.

UV (λ, nm (ε, L cm^{-1} mol^{-1})): acetonitrile: 358 (5473), 461 (5228).

4-(*tert*-Butyl)-2-((pyridin-2-ylmethylene)amino)phenolatotrichlorotin(IV) (**IV**): red finely crystalline powder, 56% yield.

For $C_{16}H_{17}Cl_3N_2OSn$

Anal. calcd., %	C, 40.17	H, 3.58	Cl, 22.23
Found, %	C, 40.35	H, 3.67	Cl, 22.02

IR (ν, cm^{-1}): 1602 s, 1526 s, 1487 s, 1365 s, 1275 s, 1241 s, 1173 s, 1155 s, 1131 s, 922 s, 839 s, 781 s.

^1H NMR ($(CD_3)_2CO$); 293 K; δ, ppm): 1.35 (s, 9H, *t*-Bu), 6.98 (d, J = 8.9 Hz, J ($^{119}Sn-^1H$) = 7.6 Hz $1H_{ar}$), 7.62 (dd, J = 8.9 Hz, J = 2.4 Hz, $1H_{ar}$), 7.94 (d, J = 2.4 Hz, $1H_{ar)}$, 8.26 (m, $1H_{Py}$), 8.52 (m, $1H_{Py}$), 8.70 (td, J = 7.8 Hz, J = 1.5 Hz, J ($^{119}Sn-^1H$) = 6.4 Hz, $1H_{Py}$), 9.18 (d, J = 5.3 Hz, J ($^{119}Sn-^1H$) = 26.8 Hz, $1H_{Py}$), 9.62 (s, J ($^{119}Sn-^1H$) = 109.0 Hz, C–H). ^{13}C NMR ($(CD_3)_2CO$); 293 K; δ, ppm): 30.5 (CH_3(*t*-Bu)), 34.1 (C(*t*-Bu)); 114.7, 119.5, 129.9, 130.4, 133.5; 134.5, 139.1, 141.4, 142.0, 144.5, 145.6 (C_{ar}); 156.9 (C=N); ^{119}Sn NMR ($(CD_3)_2CO$); 293 K; δ, ppm): –514.

UV (λ, nm (ε, L cm^{-1} mol^{-1})): acetonitrile: 352 (10346), 478(7241).

4-Chloro-2-((pyridin-2-ylmethylene)amino)phenolatotrichlorotin(IV) (**V**): orange finely crystalline powder, 35% yield.

For $C_{12}H_8N_2OCl_4Sn$

Anal. calcd., %	C, 40.17	H, 3.58	Cl, 22.23
Found, %	C, 40.32	H, 3.83	Cl, 21.98

IR (ν, cm^{-1}): 1599 s, 1590 s, 1473 s, 1289 s, 1270 s, 1239 s, 1228 s, 1173 s, 1157 s, 1119 s, 1026 s, 940 s, 875 s, 816 s, 775 s, 661 s.

^{1}H NMR ($(CD_3)_2CO$); 293 K; δ, ppm): 7.08 (d, J = 9.0 Hz $1H_{ar}$), 7.52 (dd, J = 9.0 Hz, J = 9.0 Hz, $1H_{ar}$), 8.04 (d, J = 8.7 Hz, $1H_{ar}$), 8.34 (m, $1H_{Py}$), 8.59 34 (m, $1H_{Py}$), 8.76 (td, J = 7.7Hz, J = 1.5 Hz, $1H_{Py}$), 9.22 (d, J = 5.1 Hz, $1H_{Py}$), 10.04 (s, C–H).

UV (λ, nm (ε, L cm^{-1} mol^{-1})): acetonitrile: 338 (10520), 468 (7447).

4-Nitro-2-((pyridin-2-ylmethylene)amino)phenolatotrichlorotin(IV) (**VI**): orange finely crystalline powder, 36% yield.

For $C_{12}H_8N_3O_3Cl_3Sn$

Anal. calcd., %	C, 30.84	H, 1.73	Cl, 22.76
Found, %	C, 31.02	H, 1.91	Cl, 22.49

IR (ν, cm^{-1}): 1595 s, 1571 s, 1504 s, 1483 s, 1345 s, 1300 s, 1286 s, 1255 s, 1134 s, 1028 s, 885 s, 778 s, 748 s, 657s.

^{1}H NMR ($(CD_3)_2CO$); 293 K; δ, ppm): 7.24 (d, J = 9.3 Hz $1H_{ar}$), 8.4 (m, 2H, $1H_{ar}$, $1H_{Py}$), 8.72 (d, J = 8.7 Hz, $1H_{ar}$), 8.83 (m, $1H_{Py}$), 8.96 (d, J = 2.6 Hz, $1H_{Py}$), 9.26 (d, J = 5.3 Hz, $1H_{Py}$), 10.04 (s, J(^{119}Sn–^{1}H) = 104.4 Hz, C–H); ^{13}C NMR ($(CD_3)_2CO$); 293 K; δ, ppm): 116.0, 120.1, 124.0, 129.4, 131.3, 138.9, 140.5, 143.3, 145.1, 145.2, 146.2 (C_{ar}), 163.0 (C=N);

UV (λ, nm (ε, L cm^{-1} mol^{-1})): acetonitrile: 318 (19257), 428 (8955).

2-Chloro-4-nitro-6-((pyridin-2-ylmethylene)amino)phenolatotrichlorotin(IV) (**VII**): orange finely crystalline powder, 32% yield.

For $C_{12}H_7Cl_4N_3O_3Sn$

Anal. calcd., %	C, 28.73	H, 1.41	Cl, 28.26
Found, %	C, 28.92	H, 1.63	Cl, 27.99

IR (ν, cm^{-1}): 1590 s, 1570 s, 1504 s, 1479 s, 1331 s, 1326 s, 1301 s, 1233 s, 903 s, 875 s, 776 s, 754 s, 743 s.

UV (λ, nm (ε, L cm^{-1} mol^{-1})): acetonitrile: 326 (17532), 425 (6994).

2,4-Di-*tert*-butyl-6-((phenyl(pyridin-2-yl)methylene)amino)phenolatotrichlorotin(IV) (**VIII**): violet crystals, 65% yield.

For $C_{26}H_{29}N_2OCl_3Sn$

Anal. calcd., %	C, 51.14	H, 4.79	Cl, 17.42
Found, %	C, 51.32	H, 4.90	Cl, 17.39

IR (ν, cm^{-1}): 1593 s, 1542 s, 1532 s, 1440 s, 1364 s, 1309 s, 1267 s, 1247 s, 1202 s, 1148 s, 1030 s, 999 s, 832 s, 789 s, 747 s, 697 s.

^{1}H NMR ($CDCl_3$; 293 K; δ, ppm): 0.92 (s, 9H, *t*-Bu), 1.46 (s, 9H, *t*-Bu), 6.37 (s, $1H_{ar}$), 7.37 (s, $1H_{ar}$), 7.51 (m, $2H_{ar}$), 7.62 (d, J = 7.9 Hz, $1H_{ar}$), 7.74 (m, 3H, $2H_{ar}$ and $1H_{Py}$), 7.86 (m, $1H_{Py}$), 8.18 (td, J = 7.9 Hz, J = 1.5 Hz, $1H_{Py}$), 9.28 (d, J = 5.3 Hz, $1H_{Py}$); ^{13}C NMR ($CDCl_3$; 293 K; δ, ppm): 29.3 (CH_3(*t*-Bu)), 30.6 (CH_3(*t*-Bu)), 34.0 (C(*t*-Bu)), 35.6 (C(*t*-Bu)), 116.4 (J (^{119}Sn) = 36.5 Hz), 124.6, 127.4, 127.7, 127.8, 130.3, 130.7, 131.4, 131.5, 140.14, 140.8, 143.0, 144.3, 145.1 (J (^{119}Sn) = 19.2 Hz), 146.7 (C_{ar}), 157.5 (C=N); ^{119}Sn NMR ($CDCl_3$; 293 K; δ, ppm): –507.

UV (λ, nm (ε, L cm^{-1} mol^{-1})): acetonitrile: 369 (9986), 501 (7501).

4-Methyl-2-((phenyl(pyridin-2-yl)methylene)amino)phenolatotrichlorotin(IV) (**IX**): dark red crystals, 59% yield.

For $C_{19}H_{15}Cl_3N_2OSn$

Anal. calcd., %	C, 44.54	H, 2.95	Cl, 20.76
Found, %	C, 44.75	H, 3.14	Cl, 20.43

IR (ν, cm^{-1}): 1597 s, 1536 s, 1483 s, 1444c, 1311 s, 1271 s, 1236 s, 1142 s, 1115 s, 835 s, 817 s, 788 s, 704 s.

^{1}H NMR ($(CD_3)_2CO$); 293 K; δ, ppm): 1.90 (s, 3H, CH_3), 6.16 (s, $1H_{ar}$), 6.92 (d, J = 8.5 Hz, $1H_{ar}$), 7.20 (dd, J = 8.5 Hz, J = 2.3 Hz, $1H_{ar}$), 7.65 (m, $2H_{ar}$), 7.88 (m, $3H_{ar}$), 7.98 (d, J = 8.0 Hz, $1H_{Py}$), 8.31 (m, $1H_{Py}$), 8.63 (m, $1H_{Py}$), 9.30 (d, J = 5.3 Hz, $1H_{Py}$); ^{119}Sn NMR ($(CD_3)_2CO$); 293 K; δ, ppm): –506.

UV (λ, nm (ε, L cm^{-1} mol^{-1})): acetonitrile: 352 (6420), 486 (5125).

5-Methyl-2-((phenyl(pyridin-2-yl)methylene)amino)-phenolatotrichlorotin(IV) (**X** · MeOH): red crystals, 42% yield.

For $C_{20}H_{19}Cl_3N_2O_2Sn$

Anal. calcd., %	C, 44.12	H, 3.52	Cl, 19.53
Found, %	C, 44.35	H, 3.81	Cl, 19.21

IR (ν, cm^{-1}): 1594 s, 1444 s, 1307 s, 1268 s, 1160 s, 1115 s, 984 s, 792 s, 747 s, 705 s.

^{1}H NMR ($CDCl_3$; 293 K; δ, ppm): 2.25 (s, 3H, Me), 6.25 (m, $2H_{ar}$), 6.94 (s, $1H_{ar}$), 7.49 (m, $2H_{ar}$), 7.62 (d, J = 8.0 Hz, $1H_{ar}$), 7.74 (m, 3H, $2H_{ar}$ and $1H_{Py}$), 7.89 (m, $1H_{Py}$), 8.20 (td, J = 7.8 Hz, J = 1.5 Hz, $1H_{Py}$), 9.25 (d, J = 5.2 Hz, $1H_{Py}$); ^{13}C NMR ($CDCl_3$; 293 K; δ, ppm): 22.0 (CH_3), 120.6, 120.9, 121.9, 123.2, 127.4, 127.9, 128.0, 130.8, 130.83, 131.8, 143.2, 144.0, 145.2, 146.9, 147.3 (C_{ar}), 159.9 (C=N); ^{119}Sn NMR ($CDCl_3$; 293 K; δ, ppm): −503.

UV (λ, nm (ε, L cm^{-1} mol^{-1})): acetonitrile: 362 (8164), 466 (8663).

4-(*tert*-Butyl)-2-((phenyl(pyridin-2-yl)methylene)amino)phenolatotrichlorotin(IV) (**XI**): crimson-colored finely crystalline powder, 33% yield.

For $C_{22}H_{21}Cl_3N_2OSn$

Anal. calcd., %	C, 47.65	H, 3.82	Cl, 19.18
Found, %	C, 47.84	H, 4.07	Cl, 18.97

IR (ν, cm^{-1}): 1599 s, 1536 s, 1483 s, 1366 s, 1269 s, 1249 s, 1153 s, 832 s, 706 s, 579 s.

^{1}H NMR ($CDCl_3$; 293 K; δ, ppm): 0.92 (s, 9H, *t*-Bu), 6.48 (d, J = 2.2 Hz, $1H_{ar}$), 7.06 (d, J = 8.8 Hz, $1H_{ar}$), 7.37 (dd, J = 2.2 Hz, J = 8.8 Hz, $1H_{ar}$), 7.53 (m, $2H_{ar}$), 7.66 (d, J = 7.8 Hz, $1H_{ar}$), 7.76 (m, 3H, $2H_{ar}$ and $1H_{Py}$), 7.91 (m, $1H_{Py}$), 8.21 (td, J = 7.8 Hz, J = 1.5 Hz, $1H_{Py}$), 9.28 (d, J = 5.0 Hz, $1H_{Py}$); ^{13}C NMR ($CDCl_3$; 293 K; δ, ppm): 30.6 (CH_3(*t*-Bu)), 34.0 (C(*t*-Bu)), 118.5, 120.4, 124.4, 127.5, 127.5, 127.8, 128.1, 130.8, 130.8, 131.0, 131.7, 133.7, 141.6, 143.1, 144.0, 145.3, 147.4 (C_{ar}), 158.0 (C=N); ^{119}Sn NMR ($CDCl_3$; 293 K; δ, ppm): −504.

UV (λ, nm (ε, L cm^{-1} mol^{-1})): acetonitrile: 354 (8353), 484 (6534).

4-Chloro-2-((phenyl(pyridin-2-yl)methylene)amino)-phenolatotrichlorotin(IV) (**XII**): red crystals, 36% yield.

For $C_{18}H_{12}Cl_4N_2OSn$

Anal. calcd., %	C, 40.57	H, 2.27	Cl, 26.62
Found, %	C, 40.84	H, 2.52	Cl, 26.38

IR (ν, cm^{-1}): 1592 s, 1470 s, 1308 s, 1296 s, 1266 s, 1239 s, 1228 s, 1148 s, 1032 s, 988 s, 837 s, 796 s, 746 s, 703 s, 667 s, 576 s.

^{1}H NMR ($CDCl_3$; 293 K; δ, ppm): 6.26 (d, J = 2.3 Hz, $1H_{ar}$), 7.09 (d, J = 9.0 Hz, $1H_{ar}$), 7.50 (d, J = 7.8 Hz, $2H_{ar}$), 7.76 (d, J = 7.8 Hz, $1H_{ar}$), 7.81 (m, 4H, $3H_{ar}$ and $1H_{Py}$), 7.97 (m, $1H_{Py}$), 8.26 (m, $1H_{Py}$), 9.30 (d, J = 5.4 Hz, $1H_{Py}$); ^{13}C NMR ($CDCl_3$; 293 K; δ, ppm): 121.7, 122.2, 123.4, 125.4, 127.0, 127.0, 128.4, 128.7, 129.9, 131.0, 132.2, 135.1, 136.2, 143.3, 143.6, 145.5, 149.9 (C_{ar}), 158.6 (C=N); ^{119}Sn NMR ($CDCl_3$; 293 K; δ, ppm): −503.

UV (λ, nm (ε, L cm^{-1} mol^{-1})): acetonitrile: 326 (8890), 474 (6720).

4-Nitro-2-((phenyl(pyridin-2-yl)methylene)amino)-phenolatotrichlorotin(IV) (**XIII**): orange finely crystalline powder, 48% yield.

For $C_{18}H_{12}Cl_3N_3O_3Sn$

Anal. calcd., %	C, 39.79	H, 2.23	Cl, 19.57
Found, %	C, 40.02	H, 2.46	Cl, 19.36

IR (ν, cm^{-1}): 1594 s, 1568 s, 1346 s, 1314 s, 1249 s, 1127 s, 842 s, 816 s, 801 s, 747 s, 733 s, 703 s, 658 s, 573 s.

^{1}H NMR ($(CD_3)_2CO$); 293 K; δ, ppm): 7.21 (d, J = 9.3 Hz, J (^{119}Sn—^{1}H) = 6.9 Hz, $1H_{ar}$), 7.43 (d, J = 2.7 Hz, $1H_{ar}$), 7.76 (m, $2H_{ar}$), 7.94 (m, $3H_{ar}$), 8.18 (d, J = 7.8 Hz, $1H_{Py}$), 8.26 (dd, J = 9.3 Hz, J = 2.7 Hz, $1H_{ar}$), 8.45 (m, $1H_{Py}$), 8.74 (td, J = 7.8 Hz, J = 1.5 Hz, $1H_{Py}$), 9.37 (d, J = 5.2 Hz, $1H_{Py}$); ^{13}C NMR ($(CD_3)_2CO$); 293 K; δ, ppm): 118.9, 120.3, 124.4, 126.9, 128.8, 129.6, 130.89, 130.9, 131.2, 132.6, 138.4, 142.4, 145.5, 146.0, 155.6 (C_{ar}), 163.9 (C=N); ^{119}Sn NMR ($(CD_3)_2CO$); 293 K; δ, ppm): −505.

UV (λ, nm (ε, L cm^{-1} mol^{-1})): acetonitrile: 317 (20803), 435 (9079).

2-Chloro-4-nitro-6-((phenyl(pyridin-2-yl)methylene)amino)phenolatotrichlorotin(IV) (**XIV**): yellow finely crystalline powder, 30% yield.

For $C_{18}H_{18}Cl_4N_3O_3Sn$

Anal. calcd., %	C, 37.42	H, 1.92	Cl, 24.54
Found, %	C, 37.65	H, 2.12	Cl, 24.39

IR (ν, cm^{-1}): 1595 s, 1586 s, 1514 s, 1335 s, 1310 s, 1291 s, 1227 s, 891 s, 750 s, 738 s, 696 s, 610 s.

^{1}H NMR ($(CD_3)_2CO$); 293 K; δ, ppm): 7.39 (d, J = 2.7 Hz, $1H_{ar}$), 7.79 (m, $2H_{ar}$), 7.94(m, $4H_{ar}$), 8.24 (d, J = 7.9 Hz, $1H_{ar}$), 8.36 (m, $1H_{Py}$), 8.50 (m, $1H_{Py}$), 8.77 (td, J = 7.9 Hz, J = 1.5 Hz, $1H_{Py}$) , 9.41 (d, J = 5.2 Hz, $1H_{Py}$); ^{119}Sn NMR ($(CD_3)_2CO$); 293 K; δ, ppm): −507.

UV (λ, nm (ε, L cm^{-1} mol^{-1})): acetonitrile: 320 (20090), 432 (8018).

2,4-Di-*tert*-butyl-6-((1-(pyridin-2-yl)ethylide-ne)amino)phenolatotrichlorotin(IV) (**XV**): violet finely crystalline powder, 56% yield.

For $C_{21}H_{27}Cl_3N_2OSn$

Anal. calcd., %	C, 45.98	H, 4.96	Cl, 19.39
Found, %	C, 46.15	H, 5.22	Cl, 19.11

IR (ν, cm^{-1}): 1597 s, 1476 s, 1438 s, 1367 s, 1261 s, 1245 s, 1203 s, 1168 s, 835 s, 771 s, 766 s.

^1H NMR ($CDCl_3$; 293 K; δ, ppm): 1.33 (s, 9H, *t*-Bu), 1.49 (s, 9H, *t*-Bu), 3.04 (s, 3H, CH_3), 7.44 (d, J = 1.8 Hz, $1H_{ar}$), 7.54 (d, J = 1.8 Hz, $1H_{aryl}$), 7.91 (m, $1H_{Py}$), 8.26 (d, J = 8.0 Hz, $1H_{Py}$), 8.38 (td, J = 8.0 Hz, J = 1.2 Hz, $1H_{Py}$), 9.25 (d, J = 4.8 Hz, J ($^{119}Sn-^1H$) = 27.8 Hz, $1H_{Py}$); ^{13}C NMR ($CDCl_3$; 293 K; δ, ppm): 18.2 (CH_3), 29.3 (CH_3(*t*-Bu)), 31.2 (CH_3(*t*-Bu)), 34.5 (C(*t*-Bu)), 35.6 (C(*t*-Bu)), 116.3, 125.3, 125.6, 127.7, 129.8, 140.2, 140.8, 143.4, 144.2, 145.3, 147.8 (C_{ar}), 156.5 (C=N); ^{119}Sn NMR ($CDCl_3$; 293 K; δ, ppm): −509.

UV (λ, nm (ε, L cm^{-1} mol^{-1})): acetonitrile: 357 (6773), 480 (4331).

4-Methyl-2-((1-(pyridin-2-yl)ethylidene)amino)phenolatotrichlorotin(IV) (**XVI**): red-orange finely crystalline powder, 52% yield.

For $C_{14}H_{13}Cl_3N_2OSn$

Anal. calcd., %	C, 37.34	H, 2.91	Cl, 23.62
Found, %	C, 37.62	H, 3.13	Cl, 23.39

IR (ν, cm^{-1}): 1597 s, 1548 s, 1487 s, 1447 s, 1370 s, 1291 s, 1262 s, 1246 s, 1135 s, 1028 s, 825 s, 783 s, 773 s, 591 s, 568 s.

^1H NMR ($(CD_3)_2CO$); 293 K; δ, ppm): 2.86 (s, 3H, CH_3), 3.29 (s, 3H, CH_3), 6.96 (d, J = 8.5 Hz, J ($^{119}Sn-^1H$) = 7.8 Hz, $1H_{ar}$), 7.31 (dd, J = 8.7 Hz, J = 2.3 Hz, $1H_{ar}$), 7.77 (s, $1H_{ar}$), 8.31 (m, $1H_{Py}$), 8.76 (m, $1H_{Py}$), 8.88 (d, J = 8.2 Hz, $1H_{Py}$), 9.25 (d, J = 5.3 Hz, $1H_{Py}$); ^{13}C NMR ($(CD_3)_2CO$); 293 K; δ, ppm): 17.78 (CH_3), 30.62 (CH_3), 119.2, 119.4, 119.6, 123.2, 127.8, 127.9, 129.4, 131.7, 134.9, 144.9, 145.0 (C_{ar}), 157.03 (C=N); ^{119}Sn NMR ($(CD_3)_2CO$); 293 K; δ, ppm): −507.

UV (λ, nm (ε, L cm^{-1} mol^{-1})): acetonitrile: 350 (10730), 480 (7520).

5-Methyl-2-((1-(pyridin-2-yl)ethylidene)amino)-phenolatotrichlorotin(IV) (**XVII**): orange finely crystalline powder, 48% yield.

For $C_{14}H_{13}Cl_3N_2OSn$

Anal. calcd., %	C, 37.34	H, 2.91	Cl, 23.62
Found, %	C, 37.45	H, 3.01	Cl, 23.44

IR (ν, cm^{-1}): 1610 s, 1598 s, 1586 s, 1562 s, 1480 s, 1441 s, 1366 s, 1299 s, 1263 s, 1249 s, 1166 s, 1140 s, 1120 s, 1030 s, 809 s, 774 s, 735 s, 580 s.

^1H NMR ($(CD_3)_2CO$); 293 K; δ, ppm): 2.36 (s, 3H, CH_3), 3.24 (s, 3H, CH_3, J ($^{119}Sn-^1H$) = 131.0 Hz), 6.77 (dd, J = 8.6 Hz, J = 1.9 Hz, $1H_{ar}$), 6.90 (s, $1H_{ar}$), 7.84 (d, J = 8.6 Hz, $1H_{ar}$), 8.30 (m, $1H_{Py}$), 8.75 (m, $1H_{Py}$), 8.86 (d, J = 7.9 Hz, $1H_{Py}$), 9.24 (d, J = 5.1 Hz, J ($^{119}Sn-^1H$) = 31.0 Hz, $1H_{Py}$); ^{119}Sn NMR ($(CD_3)_2CO$); 293 K; δ, ppm): −507.

UV (λ, nm (ε, L cm^{-1} mol^{-1})): acetonitrile: 349 (6807), 448 (6140).

4-(*tert*-Butyl)-2-((1-(pyridin-2-yl)ethylidene)amino)phenolatotrichlorotin(IV) (**XVIII**): red finely crystalline powder, 33% yield.

For $C_{17}H_{19}Cl_3N_2OSn$

Anal. calcd., %	C, 41.47	H, 3.89	Cl, 21.60
Found, %	C, 41.72	H, 3.99	Cl, 21.29

IR (ν, cm^{-1}): 1597 s, 1538 s, 1486 s, 1365 s, 1358 s, 1259 s, 1248 s, 1186 s, 1144 s, 1031 s, 839 s, 833 s, 778 s, 721 s.

^1H NMR ($(CD_3)_2CO$); 293 K; δ, ppm): 1.37 (s, 9H, *t*-Bu), 3.33 (s, 3H, CH_3), 7.01 (d, J = 8.9 Hz, J ($^{119}Sn-^1H$) = 7.6 Hz, $1H_{ar}$), 7.57 (dd, J = 8.9 Hz, J = 2.7 Hz, $1H_{ar}$), 7.86 (d, J = 2.4 Hz, $1H_{ar}$), 8.31 (m, $1H_{Py}$), 8.79 (td, J = 8.1 Hz, J = 1.6 Hz, $1H_{Py}$), 8.89 (d, J = 8.1 Hz, $1H_{Py}$), 9.25 (d, J = 5.4 Hz, J ($^{119}Sn-^1H$) = 31.5 Hz, $1H_{Py}$); ^{119}Sn NMR ($(CD_3)_2CO$); 293 K; δ, ppm): −507.

UV ((λ, nm (ε, L cm^{-1} mol^{-1})): acetonitrile: 342 (751), 464 (4923).

4-Chloro-2-((1-(pyridin-2-yl)ethylidene)amino)phenolatotrichlorotin(IV) (**XIX**): orange finely crystalline powder, 23% yield.

For $C_{13}H_{10}Cl_4N_2OSn$

Anal. calcd., %	C, 33.17	H, 2.14	Cl, 30.12
Found, %	C, 33.40	H, 2.28	Cl, 29.93

IR (ν, cm^{-1}): 1594 s, 1546 s, 1480 s, 1376 s, 1368 s, 1285 s, 1261 s, 1245 s, 1194 s, 1169 s, 1130 s, 1123 s, 1101 s, 1029 s, 871 s, 835 s, 827 s, 784 s, 772 s, 669 s, 590 s, 565 s.

^1H NMR ($(CD_3)_2CO$); 293 K; δ, ppm): 3.37 (s, 3H, CH_3), 7.09 (d, J = 9.0 Hz, J ($^{119}Sn-^1H$) = 7.2 Hz, $1H_{ar}$), 7.49 (dd, J = 9.0 Hz, J = 2.5 Hz, J ($^{119}Sn-^1H$) = 8.0 Hz, $1H_{ar}$), 7.95 (d, J = 2.5 Hz, $1H_{ar}$), 8.37 (m, $1H_{Py}$), 8.81 (td, J = 7.9 Hz, J = 1.6 Hz, $1H_{Py}$), 8.97 (d, J = 7.9 Hz, $1H_{Py}$), 9.27 (dd, J = 5.4 Hz, J = 1.6 Hz, $1H_{Py}$); ^{13}C NMR ($(CD_3)_2CO$); 293 K; δ, ppm): 17.7 (CH_3), 120.9, 122.2, 122.9, 126.7, 128.4, 129.0, 130.0, 133.4, 133.5, 145.1, 145.2 (C_{ar}), 157.5 (C=N); ^{119}Sn NMR ($(CD_3)_2CO$); 293 Kδ, ppm): −506.

UV (λ, nm (ε, L cm^{-1} mol^{-1})): acetonitrile: 330 (7247), 453 (4917).

X-ray diffraction analysis of complexes **I**, **VIII**–**X**, and **XII** was carried out on Bruker Smart Apex (**VIII**, **X**) and Agilent Xcalibur E (**I**, **IX**, **XII**) diffractometers

Table 1. Crystallographic data and X-ray experiment details for complexes **I**, **VIII**–**X**, and **XII**

Complex	**I**	**VIII**	**IX**	**X** · MeOH	**XII**
System	Monoclinic	Monoclinic	Monoclinic	Monoclinic	Monoclinic
Space group	$P2_1/c$	$P2_1/n$	$P2_1/n$	$P2_1/c$	$P2_1/n$
a,Å	13.9657(2)	13.2864(5)	9.21140(10)	13.5209(6)	9.1668(2)
b, Å	12.12140(10)	14.9148(5)	15.51260(10)	14.4120(6)	15.5670(3)
c, Å	14.3498(2)	13.3845(5)	13.56540(10)	22.3666(10)	13.5275(3)
β, deg	109.512(2)	96.2550(10)	98.8020(10)	103.0010(10)	98.060(2)
V, Å^3	2289.68(6)	2636.54(17)	1915.57(3)	4246.7(3)	1911.30(7)
Z	4	4	4	8	4
ρ(calcd.), Mg/m^3	1.550	1.538	1.777	1.703	1.852
μ, mm^{-1}	1.478	1.295	1.763	1.599	1.906
θ, deg	2.89–30.03	2.05–28.70	3.18–30.03	1.69–27.89	2.88–30.03
Number of observed reflections	45565	27234	69507	41573	37494
Number of unique reflections	6696	6792	5583	10116	5576
R_{int}	0.0525	0.0303	0.0284	0.0255	0.0995
$S(F^2)$	1.033	1.058	1.065	1.047	0.998
R_1/wR_2 ($I > 2\sigma(I)$)	0.0262/0.0469	0.0283/0.0652	0.0144/0.0358	0.0240/0.0558	0.0385/0.0511
R_1/wR_2 (for all parameters)	0.0374/0.0494	0.0366/0.0689	0.0151/0.0362	0.0317/0.0589	0.0643/0.0557
$\Delta\rho_{max}/\Delta\rho_{min}$), e Å^{-3}	0.468/–0.488	1.266/–0.320	0.480/–0.331	0.785/–0.369	0.891/–0.601

(ω-scan mode, MoK_α radiation, λ = 0.71073 Å, T = 100(2) K). The structures were solved by direct methods and refined by full-matrix least-squares method on F_{hkl}^2 in the anisotropic approximation for nonhydrogen atoms. The hydrogen atoms in **I**, **VIII**–**X**, and **XII** were placed into geometrically calculated positions and refined isotropically with fixed thermal parameters $U(H)_{iso} = 1.2U(C)_{eq}$ ($U(H)_{iso} = 1.5U(C)_{eq}$ for methyl groups). The integration of experimental intensity sets, absorption correction, and structure refinement were carried out using SAINT [38], SADABS [39], SHELX [40], and CrysAlisPRO [41] program packages. The crystallographic data and X-ray experiment details are summarized in Table 1 and selected bond lengths and bond angles are in Table 2.

The structures are deposited with the Cambridge Crystallographic Data Centre (no. 1849152 (**I**), 1849153 (**VIII**), 1849154 (**IX**), 1849155 (**X**), 1849156 (**XII**); http://ccdc.cam.ac.uk/getstructures).

Quantum chemical calculations for complex **I** were carried out using the Gaussian 09 program [42] by density functional theory (DFT) with the B3LYP functional [43] and the all-electron DGDZVP basis set for all atoms. The absence of imaginary frequencies indicates that the optimized molecule corresponds to the potential energy minimum.

RESULTS AND DISCUSSION

Tin complexes with Schiff bases containing an iminopyridine moiety and a phenol group capable of covalent binding to metal were prepared by template synthesis from tin tetrachloride, a variety of *o*-aminophenols and α-carbonyl-substituted pyridines. The prepared compounds contained substituents of various nature in the phenolate moiety of the ligand and at the imine carbon atom (Scheme 1). The best yields were attained for compounds containing an unsubstituted carbon atom at the imine nitrogen and electron-donating alkyl substituents in the initial aminophenol. The reactions proceed smoothly on moderate heating in a methanol solution and are completed within 20–30 min. For more complete precipitation of the intensely colored tin complexes, the reaction mixture was stirred for several hours at 50°C and cooled down to room temperature. After air-drying, the precipitated target product is analytically pure and does not require recrystallization. The products are stable to oxygen and air moisture both in the crystalline state and in solution.

Table 2. Selected bond lengths (Å) and angles (deg) in complexes **I**, **VIII**–**X**, **XII**

Bond	**I**	**VIII**	**IX**	**X**(A)	**X**(B)	**XII**
	d, Å					
Sn(1)–O(1)	2.030(2)	2.011(2)	2.0285(8)	2.031(2)	2.041(2)	2.038(2)
Sn(1)–N(1)	2.200(2)	2.209(2)	2.2017(8)	2.196(2)	2.205(2)	2.205(2)
Sn(1)–N(2)	2.229(2)	2.203(2)	2.2110(9)	2.217(2)	2.196(2)	2.212(2)
Sn(1)–Cl(1)	2.4303(5)	2.4004(5)	2.3949(3)	2.4226(5)	2.4359(6)	2.4229(7)
Sn(1)–Cl(2)	2.3486(5)	2.3466(5)	2.3506(3)	2.3441(5)	2.3347(5)	2.3528(7)
Sn(1)–Cl(3)	2.3892(5)	2.4119(5)	2.4280(2)	2.4014(5)	2.3874(6)	2.3849(8)
O(1)–C(1)	1.339(2)	1.339(2)	1.342(2)	1.339(2)	1.352(2)	1.342(3)
N(1)–C(7)	1.281(2)	1.294(3)	1.299(2)	1.289(3)	1.289(3)	1.294(3)
N(1)–C(2)	1.398(2)	1.405(3)	1.401(2)	1.409(2)	1.406(3)	1.403(4)
N(2)–C(12)	1.338(2)	1.334(3)	1.337(2)	1.331(2)	1.333(3)	1.330(4)
N(2)–C(8)	1.361(2)	1.357(3)	1.359(2)	1.360(2)	1.358(3)	1.367(3)
C(1)–C(2)	1.419(2)	1.424(3)	1.424(2)	1.416(3)	1.422(3)	1.426(4)
C(1)–C(6)	1.424(2)	1.410(3)	1.404(2)	1.402(3)	1.393(3)	1.407(4)
C(2)–C(3)	1.401(2)	1.401(3)	1.410(2)	1.401(3)	1.409(3)	1.406(4)
C(3)–C(4)	1.379(2)	1.381(3)	1.385(2)	1.376(3)	1.377(3)	1.375(4)
C(4)–C(5)	1.416(2)	1.410(3)	1.409(2)	1.401(3)	1.403(3)	1.396(4)
C(5)–C(6)	1.382(2)	1.394(3)	1.384(2)	1.389(3)	1.390(3)	1.375(4)
C(7)–C(8)	1.465(2)	1.481(3)	1.479(2)	1.482(3)	1.487(3)	1.481(4)
C(8)–C(9)	1.384(2)	1.386(3)	1.389(2)	1.386(3)	1.381(3)	1.380(4)
C(9)–C(10)	1.393(3)	1.392(3)	1.397(2)	1.392(3)	1.390(3)	1.387(4)
C(10)–C(11)	1.381(3)	1.377(3)	1.386(2)	1.380(3)	1.379(3)	1.383(4)
C(11)–C(12)	1.386(3)	1.389(3)	1.396(2)	1.386(3)	1.390(3)	1.383(4)
Angles	ω, deg					
O(1)Sn(1)N(1)	78.22(5)	78.63(6)	79.56(3)	79.45(6)	78.98(6)	79.40(8)
O(1)Sn(1)N(2)	151.84(5)	152.79(6)	153.80(3)	153.94(6)	154.11(6)	153.62(8)
N(1)Sn(1)N(2)	73.62(5)	74.19(6)	74.48(3)	74.59(6)	75.13(6)	74.42(9)
O(1)Sn(1)Cl(1)	90.38(4)	91.47(5)	92.09(3)	89.93(4)	92.69(5)	91.52(6)
N(1)Sn(1)Cl(1)	85.10(4)	91.76(5)	84.03(2)	85.81(5)	89.82(5)	83.95(6)
N(2)Sn(1)Cl(1)	87.06(4)	88.16(5)	88.72(2)	86.01(4)	87.58(5)	88.95(6)
O(1)Sn(1)Cl(2)	108.42(4)	105.21(4)	106.68(2)	105.79(4)	102.88(4)	106.62(6)
N(1)Sn(1)Cl(2)	171.99(4)	173.94(5)	172.30(2)	174.43(5)	174.38(5)	172.34(7)
N(2)Sn(1)Cl(2)	99.64(4)	101.98(4)	99.48(2)	100.09(4)	102.86(5)	99.74(6)
O(1)Sn(1)Cl(3)	91.33(4)	91.63(5)	90.49(3)	92.35(4)	91.34(5)	90.72(6)
N(1)Sn(1)Cl(3)	91.52(4)	84.81(5)	90.42(2)	89.14(5)	82.90(5)	90.38(6)
N(2)Sn(1)Cl(3)	89.63(4)	87.20(5)	86.27(2)	89.51(4)	85.21(5)	86.30(6)
Cl(1)Sn(1)Cl(2)	90.30(2)	92.81(2)	91.157(9)	92.26(2)	95.36(2)	91.08(3)
Cl(1)Sn(1)Cl(3)	175.82(2)	174.84(2)	173.352(9)	173.99(2)	170.86(2)	173.42(3)
Cl(2)Sn(1)Cl(3)	92.78(2)	90.36(2)	93.971(10)	92.47(2)	91.74(2)	94.21(3)

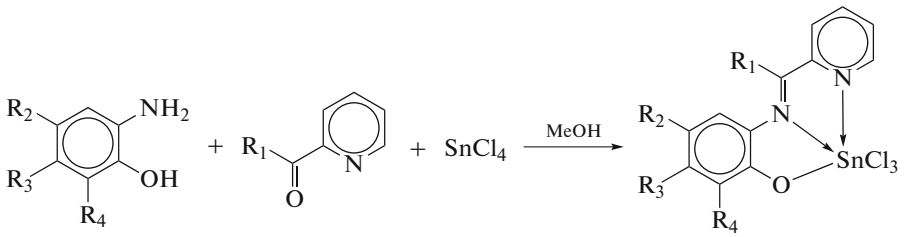

R_1 = H: R_2 = *t*-Bu, R_3 = H, R_4 = *t*-Bu **(I)**; R_2 = Me, R_3 = H, R_4 = H **(II)**; R_2 = H, R_3 = Me, R_4 = H **(III)**; R_2 = *t*-Bu, R_3 = H, R_4 = H **(IV)**; R_2 = Cl, R_3 = H, R_4 = H **(V)**; R_2 = NO_2, R_3 = H, R_4 = H **(VI)**; R_2 = NO_2, R_3 = H, R_4 = Cl **(VII)**

R_1 = Ph: R_2 = *t*-Bu, R_3 = H, R_4 = *t*-Bu **(VIII)**; R_2 = Me, R_3 = H, R_4 = H **(IX)**; R_2 = H, R_3 = Me, R_4 = H **(X)**; R_2 = *t*-Bu, R_3 = H, R_4 = H **(XI)**; R_2 = Cl, R_3 = H, R_4 = H **(XII)**; R_2 = NO_2, R_3 = H, R_4 = H **(XIII)**; R_2 = NO_2, R_3 = H, R_4 = Cl **(XIV)**

R_1 = Me: R_2 = *t*-Bu, R_3 = H, R_4 = *t*-Bu **(XV)**; R_2 = Me, R_3 = H, R_4 = H **(XVI)**; R_2 = H, R_3 = Me, R_4 = H **(XVII)**; R_2 = *t*-Bu, R_3 = H, R_4 = H **(XVIII)**; R_2 = Cl, R_3 = H, R_4 = H **(XIX)**

Scheme 1.

The obtained derivatives **I**–**XIX** are diamagnetic and contain one tridentate ONN-ligand in the monoanionic state. The composition and structure of compounds were confirmed by NMR and IR spectroscopy and elemental analysis. In all complexes, the ^{119}Sn chemical shift is in the −503 to −514 ppm range, which corresponds to six-coordinate metal, usually resonating between −125 and −525 ppm [44, 45]. It is noteworthy that poor solubility in common deuterated solvents precluded multinuclear NMR analysis of some compounds. The IR spectra exhibit strong absorption bands at 1700–1500 and 1300–1000 cm^{-1}, characteristic of double (C=N) and single bonds (C–N, C–O), respectively [46].

The molecular and crystal structures of compounds **I**, **VIII**–**X**, and **XII** were studied by X-ray diffraction (Fig. 1). The crystal cell of compound **X** comprises two independent molecules of the complex, slightly differing in the bond lengths in the organic ligand, and two solvate methanol molecules.

In all five complexes, the tin coordination polyhedron is a distorted octahedron, with organic ligand heteroatoms and one of the halogen substituents occurring in the equatorial plane. The other two chlorine ligands occupy apical positions. The tridentate ligand is virtually planar in all complexes (the mean deviation of atoms from the ligand plane does not exceed 0.07 Å) and the substituent nature has little effect on the molecular structure.

The bond length distribution in the organic ligand in compounds **I**, **VIII**–**X**, and **XII** is meaningful. The C–O bond lengths in **I**, **VIII**–**X**, and **XII** are smaller than those in the reported tin(IV) amidophenolate complexes [47–49] and are close to those in metal *o*-iminosemiquinolate derivatives [50–52]. Quinoid type distortion is observed in the aromatic phenol rings of the ligands. The C(3)–C(4) and C(5)–C(6) bonds are shorter than C(1)–C(2), C(2)–C(3), C(4)–C(5), and C(1)–C(6), which is also a typical feature of *o*-iminosemiquinlate derivatives [50–52]. The N(1)–C(2) bond is shorter than the characteristic single C–N bond, while the N(1)–C(7) bond is longer than the C=N double bond in tin complexes with coordinated neutral iminopyridine molecule [53]. This effect is attributable to conjugation of the π-system of the iminopyridine group of the ligand with the π-system of its phenolate moiety, resulting in negative charge delocalization over the whole organic ligand and in the corresponding bond length redistribution.

In all five complexes studied by X-ray diffraction, the metal–oxygen and metal–nitrogen bond length distribution corresponds to the structural formula depicted in the Scheme. The Sn(1)–O(1) distances (2.011(2)–2.041(2) Å) are shorter than the sum of the Sn and O covalent radii (2.11 Å) [54] and correspond to the metal–oxygen covalent bond. The Sn(1)–N(1) and Sn(1)–N(2) distances (2.196(2)–2.229(2) Å) are somewhat greater than the sum of the covalent radii (2.12 Å) [54], but markedly smaller than the sum of van der Waals radii of Sn and N (3.8 Å) [54], which is indicative of the donor-acceptor coordination binding of these elements. In complexes **I**, **IX**, and **X**(A), the Sn(1)–N(1) bonds (2.196(2)–2.2017(8) Å) with imine nitrogens are somewhat shorter than the Sn(1)–N(2) bond (2.2110(9)–2.229(2) Å) with pyridine, which was observed previously for analogous tin complexes with this type of ligands [34–36].

In order to understand the causes for the considerable change in the positions of the UV/Vis bands and, hence, the color differences between complexes **I**–**XIX**, we carried out quantum chemical calculations for complex **I** by the density functional theory method. From analysis of the molecular orbitals of the optimized molecule, one can conclude that the lowest unoccupied molecular orbital (LUMO) and the highest occupied molecular orbital (HOMO) are almost

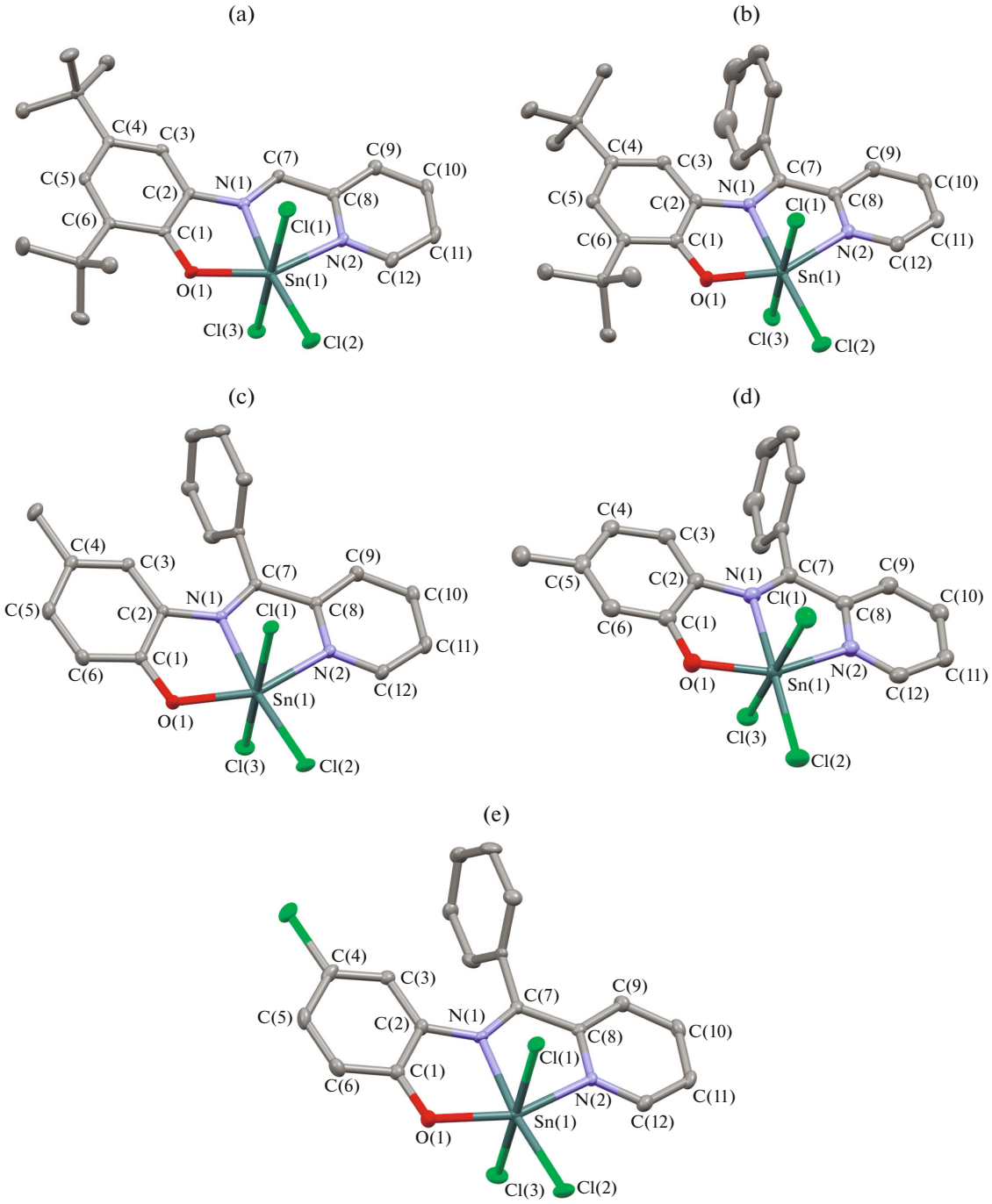

Fig. 1. Molecular structure of (a) **I**, (b) **VIII**, (c) **IX**, (d) **X**, (e) **XII**. The thermal ellipsoids are given at 50% probability level. The hydrogen atoms are omitted for clarity.

completely concentrated on the organic ligand (Fig. 2). Thus, the HOMO–LUMO gap determines the position of the long-wavelength peak in the UV/Vis spectrum, corresponding to the interligand charge transfer (ILCT). According to calculations, the energy gap between the frontier orbitals of **I** is 2.57 eV (λ = 483 nm), which is consistent with experimental data (λ = 494 nm in acetonitrile). The HOMO of complex **I** is localized on the donor amidophenolate moiety of the ligand, while the LUMO is on the acceptor iminopyridine moiety (Fig. 2). The introduction of various substituents into the organic ligand affects the energy gap between the frontier orbitals and, hence, the positions of UV/Vis peaks. Electron-withdrawing substituents in the iminopyridine moiety should reduce the LUMO energy and thus induce a red shift

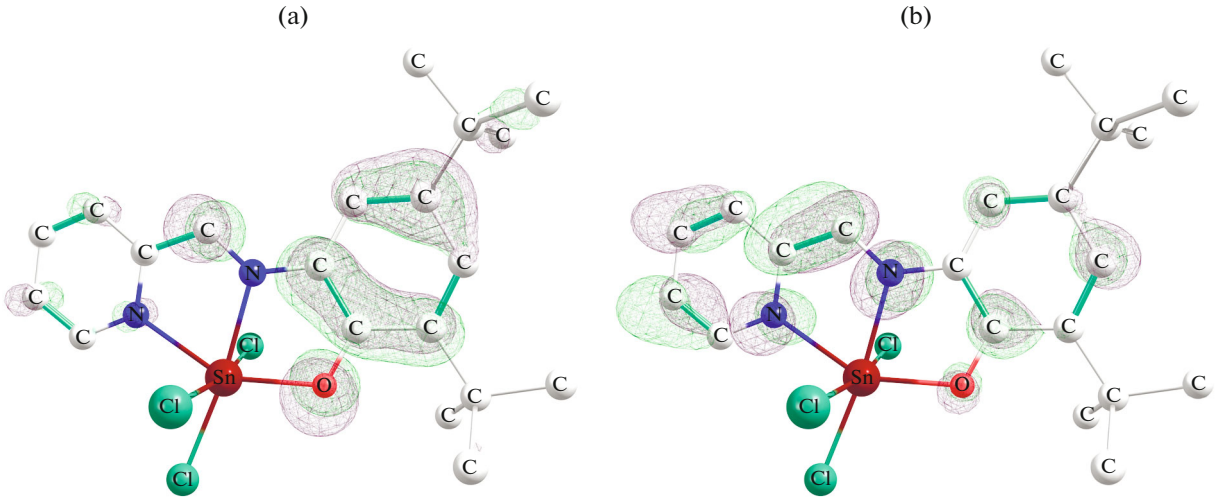

Fig. 2. Shape of the frontier orbitals, (a) HOMO and (b) LUMO, of complex **I** according to DFT data. The hydrogen atoms are omitted.

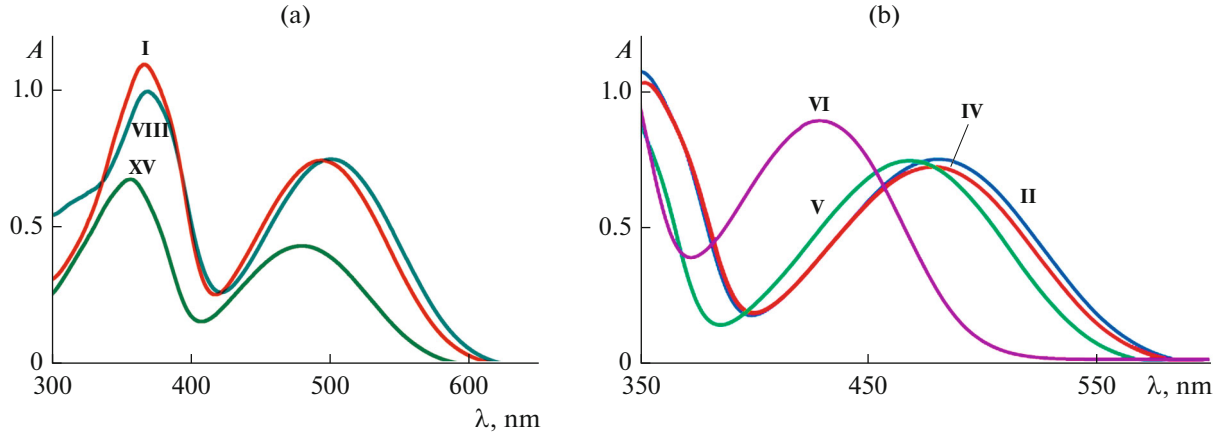

Fig. 3. UV/Vis spectra of complexes (a) **I**, **VIII**, and **XV** and (b) **II**, **IV**, **V** and **VI** in acetonitrile. $c = 1 \times 10^{-4}$mol/L.

of the absorption band. Consider complexes **I**, **VIII**, and **XV** containing organic ligands with identical substituents in the phenolic moiety but different substituents (R_1) at the imine carbon atom. An unambiguous red shift is observed on going from the electron-donating methyl group to hydrogen or to phenyl group (λ = 480 (R_1 = Me), 494 (R_1 = H), 501 (R_1 = Ph) nm (Fig. 3a)).

An opposite effect is induced by enhancement of electron-withdrawing properties of substituents in the phenolic moiety of the organic ligand. Electron-withdrawing groups should reduce the HOMO energy and thus induce a blue shift in the UV/Vis spectrum. Figure 3b shows the spectra of complexes **II** and **IV**–**VI**. These compounds contain different substituents (R_2) in position 5 of the phenolic moiety and invariable substituent R_1 = H. The presence of stronger electron-withdrawing groups R_2 shifts the UV/Vis absorption peaks to shorter wavelength (λ = 480 (R_2 = Me), 478 (R_2 = *t*-Bu), 468 (R_2 = Cl), 428 (R_2 = NO_2) nm). A similar blue shift in the UV/Vis spectrum upon enhancement of the electron-withdrawing properties of substituents in the phenolic moiety was found for salicyldiimine complexes of aluminum [55] and indium [56].

Compounds exhibiting intramolecular charge transfer are known to be subject to solvatochromism [37]. The influence of solvents on the UV/Vis spectra was considered in relation to complex **I**. Indeed, on going from acetonitrile to toluene, a red shift of the long-wavelength band by 28 nm is observed. However, no unambiguous correlation can be found between the absorption band shift and the empirical solvent polarity parameter [37]. This implies that specific interactions related to tin atom solvation with solvent molecules occur in solutions. Previously, the possibility of

this solvation was identified for six-coordinate tin complexes containing a similar diiminodiphenolate ligand [57].

Thus, this study demonstrated the applicability of template assembly for targeted synthesis of metal complexes with Schiff bases containing an iminopyridine moiety. A series of new six-coordinate tin(IV) complexes based on tridentate ONN-ligands were obtained by one-step synthesis. The influence of electron-withdrawing (electron-donating) properties of substituents in various organic ligand groups on the UV/Vis spectra of the compounds was demonstrated. This gives a convenient tool for the targeted design of chromophore compounds with fine-tuned photophysical characteristics.

ACKNOWLEDGMENTS

This study was performed as a part of Government Order (Subject no. 44.1, no. AAAA-A16-116122110056-2).

REFERENCES

1. Andruh, M., *Dalton Trans.*, 2015, vol. 44, p. 16633.
2. Cozzi, P.G., *Chem. Soc. Rev.*, 2004, vol. 33, p. 410.
3. Grusenmeyer, T.A., King, A.W., Mague, J.T., et al., *Dalton Trans.*, 2014, vol. 43, p. 17754.
4. Kumar, S. and Nath, M., *J. Organomet. Chem.*, 2018, vol. 856, p. 87.
5. Baula, T.S.B., Kehie, P., Duthie, A., et al., *J. Organomet. Chem.*, 2017, vol. 828, p. 96.
6. Bhatr, P., Sharma, J., Sharma, R.A., and Singh, Y., *Appl. Organomet. Chem.*, 2018, vol. 31, p. 3639.
7. Vinayak, R., Dey, D., Ghosh, D., et al., *Appl. Organomet. Chem.*, 2018, vol. 32, p. 4122.
8. Baul, T.S.B., Longkumer, I., Duthie, A., et al., *Dalton Trans.*, 2018, vol. 47, p. 1993.
9. Galvan-Hidalgo, J.M., Chans, G.M., Ramirez-Apan, T., et al., *Appl. Organomet. Chem.*, 2018, vol. 31, p. 3704.
10. Zafarian, H., Sedaghat, T., Motamedi, H., et al., *J. Organomet. Chem.*, 2017, vol. 853, p. 184.
11. Ahlawat, A., Singh, V., and Asija, S., *Chem. Papers*, 2017, vol. 71, p. 2195.
12. Devi, J. and Pachwania, S., *Inorg. Chem. Commun.*, 2018, vol. 91, p. 44.
13. Liu, K., Chang, G.L., Yan, H., et al., *Appl. Organomet. Chem.*, 2018, vol. 32, p. 3973.
14. Kovala-Demertzi, D., *J. Organomet. Chem.*, 2006, vol. 691, p. 1767.
15. Vinsova, J., Cermakova, K., Tomeckova, A., et al., *Bioorg. Med. Chem.*, 2006. vol. 14, no. 17, p. 5850.
16. Tian, L.J., Yao, Y.Z., Wang, Y.H., and Liu, J., *J. Mol. Struct.*, 2018, vol. 1156, p. 441.
17. Enriquez-Cabrera, A., Vega-Penaloza, A., Alvarez-Venicio, V., et al., *J. Organomet. Chem.*, 2018, vol. 855, p. 51.
18. Hazra, S., Martins, N.M.R., Kuznetsov, M.L., et al., *Dalton Trans.*, 2017, vol. 46, p. 13364.
19. Martins, L.M.D.R.S., Hazra, S., da Silva, M.F.C.G., Pombeiro, A.J.L., *RSC Adv.*, 2016, vol. 6, p. 78225.
20. Garcia-Lopez, M.C., Munoz-Flores, B.M., Chan-Navarro, R., et al., *J. Organomet. Chem.*, 2016, vol. 806, p. 68.
21. Majumder, A., Rosair, G., Mallick, A., Chattopadhyay, N., and Mitra, S., *Polyhedron*, 2006, vol. 25, no. 8, p. 1753.
22. Stefankiewicz, A., Wałesa-Chorab, M., Szczesniak, H., et al., *Polyhedron*, 2010, vol. 29, no. 1, p. 178.
23. Maheswari, P., Hartl, F., Quesada, M., et al., *Inorg. Chim. Acta*, 2011, vol. 374, no. 1, p. 406.
24. Ma, S., Sun, X., Gao, S., et al., *Eur. J. Inorg. Chem.*, 2007, no. 6, p. 846.
25. Qiao, X., Ma, Z., Xie, C., et al., *J. Inorg. Biochem.*, 2001, vol. 105, no. 5, p. 728.
26. Pursche, D., Triller, M., Reddig, N., et al., *Z. Anorg. Allg. Chem.*, 2003, vol. 629, no. 1, p. 24.
27. Qi, C., Sun, X., Gao, S., et al., *Eur. J. Inorg. Chem.*, 2007, no. 23, p. 3663.
28. Hayami, S., Gu, Z., Shiro, M., et al., *J. Am. Chem. Soc.*, 2000, vol. 122, no. 29, p. 7126.
29. Hayami, S., Hiki, K., Kawahara, T., et al., *Chem.-Eur. J.*, 2009, vol. 15, no. 14, p. 3497.
30. Gomez-Blanco, N., Fernandez, J., Fernandez, A., et al., *Eur. J. Inorg. Chem.*, 2009, no. 21, p. 3071.
31. Epstein, D., Choudhary, S., Churchill, M., et al., *Inorg. Chem.*, 2001, vol. 40, no. 7, p. 1591.
32. Bacchi, A., Carcelli, M., Pelizzi, C., et al., *Eur. J. Inorg. Chem.*, 2002, no. 8, p. 2179.
33. Ramírez-Jiménez, A., Luna-García, R., Cortés-Lozada, A., et al., *J. Organomet. Chem.*, 2013, vol. 738, p. 10.
34. Teo, S.-B., Teo, H.-SH., Chang, S.T., et al, *J. Coord. Chem.*, 2000, vol. 49, p. 269.
35. Ramírez-Jiménez, A., Gómez, E., and Hernández, S., *J. Organomet. Chem.*, 2009, vol. 694, p. 2965.
36. Piskunov, A.V., Trofimova, O.Y., Piskunova, M.S., et al., *Russ. J. Coord. Chem.*, 2018, vol. 44, p. 138. doi 10.1134/S1070328418020082
37. Reichardt, C. and Welton, T., *Solvents and Solvent Effects in Organic Chemistry*, Berlin: VCH, 1988.
38. *SAINT*, Madison: Bruker AXS Inc., 2012.
39. Krause, L., Herbst-Irmer, R., Sheldrick, G.M., et al., *J. Appl. Crystallogr.*, 2015, vol. 48, p. 3.
40. Sheldrick, G.M., *Acta Crystallogr., Sect C: Struct. Chem.*, 2015, vol. 71, p. 3.
41. *Agilent. CrysAlis PRO*, Yarnton (Oxfordshire, England): Agilent Technologies Ltd., 2014.
42. Frisch, M.J., Trucks, G.W., Schlegel, H.B., et al., *Gaussian 09. Revision D.01*, Wallingford (CT, USA): Gaussian, Inc., 2013.
43. Becke, A.D., *J. Chem. Phys.*, 1986, vol. 84, p. 4524.
44. Wrackmeyer, B., *Annu. Rep. NMR Spectrosc.*, 1985, vol. 16, p. 73.
45. Wrackmeyer, B., *Annu. Rep. NMR Spectrosc.*, 1999, vol. 38, p. 203.

46. Gordon, A. and Ford, R., *The Chemist's Companion: A Handbook of Practical Data, Techniques, and References*, New York: Wiley, 1972.

47. Piskunov, A.V., Chegerev, M.G., and Fukin, G.K., *J. Organomet. Chem.*, 2016, vol. 803, no. 1, p. 51.

48. Chegerev, M.G., Piskunov, A.V., Maleeva, A.V., et al., *Eur. J. Inorg. Chem.*, 2016, p. 3813.

49. Chegerev, M.G., Piskunov, A.V., Starikova, A.A., et al., *Eur. J. Inorg. Chem.*, 2018, no. 9, p. 1087.

50. Piskunov, A.V., Aivaz'yan, I.A., Abakumov, G.A., et al., *Russ. Chem. Bull.*, 2007, vol. 56, no. 2, p. 261.

51. Piskunov, A.V., Meshcheryakova, I.N., Baranov, E.V., et al., *Russ. Chem. Bull.*, 2010, vol. 59, no. 2, p. 361.

52. Piskunov, A.V., Mescheryakova, I.N., Fukin, G.K., et al., *Heteroatom Chem.*, 2009, vol. 20, no. 6, p. 332.

53. Basu, B.S., Basu, B.T.S., and Tiekink, E.R.T., *Z. Kristallogr.*, 1999, vol. 214, p. 207.

54. Batsanov, S.S., *Zh. Neorg. Khim.*, 1991, vol. 36, no. 12, p. 3015.

55. Lee, S.H., Shin, N., Kwak, S.W., et al., *Inorg. Chem.*, 2017, vol. 56, p. 2621.

56. Hwang, K.Y., Lee, Y.S., Lee, M.H., and Do, Y., *Chem.-Eur. J.*, 2009, vol. 15, p. 6478.

57. Piskunov, A.V., Trofimova, O.Yu., Fukin, G.K., et al., *Dalton Trans.*, 2012, vol. 41, p. 10970.

Translated by Z. Svitanko